Analytical Model for the Four-Point Double-Toggle Mechanism during the Real Mold Clamping Process

Wen-Yi Lin
Assistant Professor, Department of Mechanical Engineering, De Lin Institute of Technology

Abstract

In this study, a simple kineto-elastostatic model for the necessary thrust applied to the crosshead of the four-point double-toggle mechanism during the real mold clamping operation is proposed to investigate the effects of the deformation of the toggle links and the hinge friction. The friction is considered to be the Coulomb friction. A practical example is studied for different values of coefficient of friction to investigate the two effects. The two effects should not be neglected during the real mold clamping operation. The maximum thrust is underestimated if the effect of the deformation of the toggle links is neglected.

Keywords: injection-molding machine, four-point double-toggle clamping mechanism, hinge friction

四點式雙肘節機構在真正合模過程中之解析模式

林文一
德霖技術學院機械工程系 助理教授

摘　要

本文使用一個簡單的運動彈性靜力模型來推導四點式雙肘節合模機構在真正合模過程中十字頭所需之推力以調查肘節連桿的變形效應以及旋轉接頭處的摩擦效應。假設在真正合模過程中旋轉接頭處的摩擦可以採用庫倫摩擦。在各種不同摩擦係數下之實際四點式雙肘節合模機構的模擬將可顯示這兩者的效應是不可以忽略的。若忽略肘節連桿的變形效應將會低估十字頭所需的最大推力。

關鍵字：射出成型機、四點式雙肘結合模機構、銷接頭摩擦

I. Introduction

The adoption of the five-point double-toggle mechanism is for the consideration of a larger opening stroke in the design of a mold-clamping mechanism of an injection-molding machine (or a die-cast machine). On the other hand, the adoption of the four-point double-toggle mechanism, as shown in Fig. 1, is for the consideration of thrust saving in design. In Fig. 1, an upper portion above a centerline CL of each mold clamping mechanism illustrates a mold closing state with the toggle fully extended in a straight line (but no real mold clamping), while a lower portion below the centerline CL illustrates the maximum stroke of mold opening of each mold clamping mechanism.

It is well known that the ideal mechanical advantage becomes infinity for the toggle clamping mechanism free from the action of friction in pin joints (hinge friction) when the toggle is fully extended in a straight line. However, in practice, the existence of the hinge friction diminishes the mechanical advantage. The necessary input force for selecting the size of the clamping cylinder or servo electric motor should be directly based on the necessary thrust applied to the crosshead during the real mold clamping. If the necessary thrust applied to the crosshead cannot be determined with more accuracy, the clamping cylinder diameters or rated output capacities of clamping servo electric motors may be overestimated or underestimated. To determine the necessary thrust applied to the crosshead with more accuracy, the hinge friction and the deformations of the tie bars and the toggle links should be taken into account.

The purpose of this paper is to investigate the effect of the deformation of the toggle links of the four-point double-toggle mechanism and the effect of the hinge friction during the real mold clamping operation. A simple kineto-elastostatic model for the necessary thrust applied to the crosshead of the four-point double-toggle clamping mechanism during the real mold clamping operation is proposed to investigate the two effects.

Lubrication of the joints is crucial to the satisfactory operation of the toggle clamping mechanism (Smith, 1995). Hydrodynamic lubrication between toggle pins and bushings cannot be achieved due to the reciprocating motion of the toggle mechanism and heavy contact forces (Huang, 1988). The lubrication between the two members may be considered as boundary or thin-film lubrication (Huang, 1988). A partial breakdown of a thin oil or grease film between the two members usually occurs during the real mold clamping, because of heavy forces. Such situation may cause direct physical contact and rubbing between two metal members. This type of friction may be considered as Coulomb friction. Conservatively, it may be reasonable to assume that Coulomb friction in pin joints is valid for the real mold clamping operation, as adopted by Burton (1979).

II. Simple kineto-elastostatic model

The degree of freedom for the four-point double-toggle mechanism is one, which can be obtained from Gruebler-type formulas (Burton, 1979). Let members 1 to 8 shown in Fig. 1 denote moving-platen-side links (1), tailstock-platen-side links (2), crosshead links (3), crosshead (4), tailstock platen (5), moving platen (6), tie bars (7), and stationary platen (8), respectively, for a four-point double-toggle clamping mechanism throughout this study. Points A to E denote centers of pin joints. A stationary platen 8 fixed to the injection-molding machine frame, and four tie bars 7 are immovably fixed to the four corners of the stationary platen, individually. A tailstock platen 5, mounted on the precision ground steel brand fixed on the frame, is attached to the respective end portions of the tie bars. A moving platen 6, mounted by the support blocks or rollers on the precision ground steel brand fixed on the frame, is slidably fitted on the tie bars. As two sets of toggle links, which are formed of links 1 (moving-platen-side links) and links 2 (tailstock-platen-side links), are bent or stretched synchronously, the moving platen moves toward or away from the tailstock platen. A crosshead 4, which is movable straight in the mold opening or closing direction by means of a drive mechanism composed of a ball nut-screw or hydraulic ram, is provided in a position (on the centerline of a machine) intermediate between the two sets of toggle links that are vertically juxtaposed so as to be bendable toward each other. The respective distal ends of two sets of crosshead links 3 that are pivotally mounted on the upper and lower sides of the crosshead, individually, pull in or push out joint portions of the toggle links, depending on the moving direction of the crosshead, whereupon the mold opening or closing operation is performed. In the last stage of mold closing operation, the tailstock platen will move away from the moving platen and the tie bars will be stretched after the contact between the moving mold attached to the moving platen and the stationary mold attached to the stationary platen. This part of mold closing operation is called the real mold clamping in this paper. Note that to prevent mold damage, the velocity of the crosshead in the stage with the contact between the moving mold and the stationary mold is always reduced to very low.

In the process of the real mold clamping, in order to develop the clamping force, the toggle clamping mechanism must overcome the friction forces in pin joints and slider connections, and the total deformation force of the tie bars. Here, the slider connections comprise the crosshead and the guide rods, and the tailstock platen and the precision ground steel bands. In practice, the design of the toggle mold clamping mechanism tends toward rugged. However, the effect of the toggle linkage deformation should be considered unless the stiffness of the toggle linkage is very much greater than that of the tie bars. In this paper, only the real mold clamping operation is considered, and the following assumptions are made:

(1) The axial deformation displacements of links and tie bars are small, and the flexural deformations of links are negligible.

(2) The inertia forces, the weights, and the friction forces in the slider connections can be neglected when compared to the total deformation force of the tie bars and the thrust of the crosshead.

(3) The deformation effects of the mold and the mold platens are negligible.

(4) Coulomb friction is valid for the friction in pin joints.

Due to assumption (1), the equilibrium equations of the toggle clamping system are constructed at the undeformed configuration of the toggle clamping system during the real mold clamping operation in this study.

Figure 2 depicts a skeleton drawing for the lower half of the four-point double-toggle clamping mechanism during the real mold clamping operation. The dashed lines denote the configuration when the moving platen is just in contact with the stationary platen. It is assumed that the toggle mechanism and the tie bars are not yet deformed in this configuration. After the contact, the toggle linkage is subjected to compressive force. Thus, besides the rigid body motion, there arises the compressive deformation for the toggle linkage. As can be seen from the solid line shown in Fig. 2, the moving platen is at rest and the tailstock platen moves backward after the contact. The final position of the real mold clamping operation is achieved when the toggle is fully extended in a straight line. In this paper, the symbol ($\tilde{\ }$) denotes that the quantity in parentheses is in the state of the final position of mold clamping operation.

From Fig. 2 and the geometry of the final position of the real mold clamping operation and the assumption of small deformation, one can have

$$L_2\sin\alpha_c - L_1\sin(\pi-\beta_c) = (L_2-\delta_{BC})\sin\alpha - (L_1-\delta_{AB})\sin(\pi-\beta) = d_A, \tag{1}$$

$$L_2\sin\alpha_c + L_3\sin(\pi-\phi_c) = (L_2-\delta_{BC})\sin\alpha + (L_3-\delta_{BE})\sin(\pi-\phi) = d_E, \tag{2}$$

$$\tilde{\beta} = \tilde{\alpha} + \pi, \tag{3}$$

$$\begin{aligned} U_C &= (L_1-\delta_{AB})\cos(\pi-\beta) - L_1\cos(\pi-\beta_c) + (L_2-\delta_{BC})\cos\alpha - L_2\cos\alpha_c \\ &= \overline{U}_C - \delta_{AB}\cos(\pi-\beta) - \delta_{BC}\cos\alpha \end{aligned}, \tag{4}$$

$$\overline{U}_C = L_1[\cos(\pi-\beta) - \cos(\pi-\beta_c)] + L_2(\cos\alpha - \cos\alpha_c), \tag{5}$$

$$U_E = L_3\cos(\pi-\phi_c) - (L_3-\delta_{BE})\cos(\pi-\phi) + L_1\cos(\pi-\beta_c) - (L_1-\delta_{AB})\cos(\pi-\beta) \tag{6}$$

where L_i (i = 1 - 3) are the distances between joins A and B, B and C, and B and E, respectively, at the undeformed state of the mechanism; U_C is the displacement of the tailstock platen; δ_{AB}, δ_{BC} and δ_{BE} are the axial shortened lengths of links 1, 2 and the crosshead link, respectively. Due to assumption of small deformation, δ_{AB}, δ_{BC}, and δ_{BE} in equations (1), (2) and (6) are dropped in this study. Thus, one can obtain the values of $\tilde{\alpha}$, $\tilde{\beta}$ and $\tilde{\phi}$ using Eqs. (1) - (3).

During the real mold clamping process, the links 1, links 2 and the crosshead links are subjected to forces F_1, F_2, and F_3, respectively, as shown in Fig. 3. The circles shown in Fig. 3 are called friction circles (Burton, 1979; Wilson et al., 1983). For the sake of clarity, the friction circles in Fig. 3 have been greatly exaggerated in magnitude. From Fig. 1 and Fig. 3, the free-body diagrams for each member and joint can be easily drawn (not shown), and the equations of equilibrium required for the real mold clamping operation are given as follows.

$$F_{cl} = F_1\cos(\pi-\beta+\beta_\mu), \tag{7}$$

$$F_o = F_3\cos(\pi-\phi-\phi_\mu), \tag{8}$$

$$F_c = F_2 \cos(\alpha + \alpha_\mu), \tag{9}$$

$$F_1 \sin(\pi - \beta + \beta_\mu) + F_2 \sin(\alpha + \alpha_\mu) - F_3 \sin(\pi - \phi - \phi_\mu) = 0, \tag{10}$$

$$F_1 \cos(\pi - \beta + \beta_\mu) - F_2 \cos(\alpha + \alpha_\mu) - F_3 \cos(\pi - \phi - \phi_\mu) = 0, \tag{11}$$

$$\alpha_\mu = \sin^{-1}(\frac{2\rho_B}{L_2}), \quad \beta_\mu = \sin^{-1}(\frac{2\rho_B}{L_1}), \quad \phi_\mu = \sin^{-1}(\frac{\rho_B + \rho_E}{L_3}), \tag{12}$$

$$\rho_B = \frac{\mu}{\sqrt{1+\mu^2}} r_B, \quad \rho_E = \frac{\mu}{\sqrt{1+\mu^2}} r_E, \tag{13}$$

where F_{cl} is the clamping force; F_o is the thrust transmitted to the crosshead; F_c is the total tension force of the tie bars; μ is the friction coefficient in pin joints; r_B, and r_E are the radiuses of pin joints B, and E, respectively; and ρ_B, and ρ_E are the corresponding friction radiuses, respectively. Note that in practice, the radiuses of joint A, joint B, and joint C are equal.

From Eq. (7) and Fig. 3, the compressive axial force in a single link 1 can be expressed as

$$F_{AB} = \frac{F_{cl} \cos\beta_\mu}{n_1 \cos(\pi - \beta + \beta_\mu)}, \tag{14}$$

where n_1 is the number of links 1.

From Eq. (9) and Fig. 3, the compressive axial force in a single link 2 can be expressed as

$$F_{BC} = \frac{F_c \cos\alpha_\mu}{n_2 \cos(\alpha + \alpha_\mu)}, \tag{15}$$

where n_2 is the number of links 2.

From equations (14) - (15), δ_{AB} and δ_{BC}, the axial shortened length of links 1 and 2 defined in Eq. (4), can be expressed by

$$\delta_{AB} = \frac{F_{AB} L_1}{A_1 E_1}, \tag{16}$$

$$\delta_{BC} = \frac{F_{BC} L_2}{A_2 E_2}, \tag{17}$$

where A_i and E_i (i = 1, 2) are the cross-sectional area and Young's modulus of links 1 and 2, respectively.

The elongation of the tie bars, equal to the displacement U_C of the tailstock platen according to the condition of geometric compatibility, can be expressed by

$$U_C = \frac{F_c L_c}{n_c A_c E_c}, \tag{18}$$

where F_c is the total tension of all tie bars given in Eq. (15); L_c is the length of the tie bar; n_c is the number of the tie bar; A_c and E_c are the cross-sectional area and Young's modulus of the tie bar, respectively.

Substituting Eqs. (16) – (18) into Eq. (4), one can obtain

$$\frac{F_c L_c}{n_c A_c E_c} + \frac{F_{AB} L_1}{A_1 E_1} \cos(\pi - \beta) + \frac{F_{BC} L_2}{A_2 E_2} \cos\alpha = \overline{U}_C. \tag{19}$$

Using Eqs. (7), (8), (10), and (11), one can obtain the mechanical advantage M_a of the four-point double-toggle mold-clamping mechanism as

$$M_a = \frac{F_{cl}}{F_o} = \frac{\tan(\alpha + \alpha_\mu) + \tan(\pi - \phi - \phi_\mu)}{\tan(\alpha + \alpha_\mu) + \tan(\pi - \beta + \beta_\mu)} . \tag{20}$$

From Eqs. (7), (8), (9), and (11), one can obtain

$$F_c + F_o = F_{cl} . \tag{21}$$

Substituting Eqs. (14) and (15) into Eq. (19), one can obtain the relation among the total deformational force of the tie bars F_c, the clamping force F_{cl}, and the necessary thrust applied to the crosshead F_o from Eqs. (19), (20), and (21).

For a specified final total deformational force of the tie bars, the final clamping force and the thrust of the crosshead can be obtained from Eqs. (20) and (21). Then, the final deformations for links 1, 2 and tie bars can be calculated from equations (16) – (18). Then, using Eqs. (1), (2), (4) and (5), one can determine the values of α_c, β_c, and ϕ_c required at the beginning of the real mold clamping operation. The nonlinear equation in this study can be solved using the bisection method.

III. Illustrative example

A practical example of four-point double-toggle mechanism with clamping force 1,350 metric tons is studied. The geometric properties are as follows: $L_1 = 1056$ mm, $A_1 = 21000$ mm^2, $n_1 = 12$ for links 1; $L_2 = 880$ mm, $A_2 = 21000$ mm^2, $n_2 = 12$ for links 2; $L_3 = 628.12$ mm for links 3; $L_c = 5800$ mm, $A_c = 85530$ mm^2, $n_c = 4$ for the tie bars; $d_A = 200$ mm, $d_E = 717.5$ mm, $r_B = 75$ mm, $r_E = 50$ mm. Young's modulus of the toggle links made of ductile irons is 17593 kgf/mm^2, and Young's modulus of the tie bars made of Cr-Mo steels is 20800 kgf/mm^2. In the example, $\tilde{\alpha} = 5.93^\circ$, $\tilde{\beta} = 185.93^\circ$, and $\tilde{\phi} = 94.0^\circ$, when the final clamping position is achieved.

To investigate the influence of the hinge friction on the necessary thrust of the crosshead, the final total deformational force of the tie bars $\tilde{F}_c = 1{,}300$ metric tons is considered, and different values of the frictional coefficient μ are considered. The value of α_c corresponding to $\tilde{F}_c = 1{,}300$ metric tons is 8.50°. The values of $\tilde{U}_C$ and $\tilde{U}_E$ are 1.06 mm and 181.99 mm, respectively, for $\mu = 0$. Fig. 4 shows the curves of the total deformation force F_c of the tie bars versus angle α. Fig. 5 shows the curves of mechanical advantage M_a versus angle α for several friction coefficients. Fig. 6 shows the curves of necessary thrust F_o applied to the crosshead versus angle α for several friction coefficients. As can be seen from Figs. 4 - 6, one may see the fundamental characteristics of the toggle clamping system during real mold clamping explained in the followings. The necessary thrust applied to the crosshead increases rapidly after the occurrence of real mold clamping, and decreases rapidly after reaching the maximum value. Thus, the position for the maximum thrust is neither at the initial position of real mold clamping nor at the final position. At the beginning of real mold clamping, the rate of increase of the mechanical advantage is slow in comparison with the rate of increase of the deformational force of the tie bars. Thus, the thrust of the crosshead increases dramatically at the beginning. But after a particular position, the rate of increase of the mechanical advantage is up in contrast to the slowdown of the rate of increase of the deformational force of the tie bars, along with reduction of angle α . Thus, the thrust applied to the crosshead decreases after the particular position. Therefore, the thrust of the crosshead has a maximum value $F_{o,\max}$ during real mold clamping. In the absence of hinge friction, the maximum thrust of the crosshead is 11.963 metric tons. The maximum thrusts of the crosshead are 12.756, 16.107, 20.659, 25.554 and 30.731 metric tons for frictional coefficients 0.01, 0.05, 0.10, 0.15, and 0.20, respectively. Thus, the effect of the hinge friction should not be neglected for real mold clamping operation. Note that the thrust of the crosshead is not zero at the final clamping position. Fig. 7 shows that the necessary thrust F_o with angle α for several frictional coefficients under considering and neglecting the deformational effect of the toggle links. The relation between the maximum thrust $F_{o,\max}$ and the friction coefficient μ under considering and neglecting the deformational effect of the toggle links is shown in Fig. 8. It can be seen from Figs. 7 and 8 that the necessary thrust of the crosshead may be underestimated, if the deformational effect of the toggle links is neglected. The maximum thrusts of the crosshead are underestimated to be 9.421, 12.445, 16.598, 21.102, and 25.894 metric tons for frictional coefficients 0.01, 0.05, 0.10, 0.15, and 0.20, respectively. If the both effects are neglected, the maximum thrusts are underestimated to be 8.711 metric tons.

IV.Conclusions

The simple kineto-elastostatic model for the necessary thrust applied to the crosshead of the four-point double-toggle clamping mechanism during real mold clamping operation is proposed with the consideration of Coulomb friction. As can be seen from the present results, the necessary thrust applied to the crosshead increases rapidly after the occurrence of real mold clamping, and decreases rapidly after reaching the maximum value. The position for the maximum thrust is neither at the initial position of real mold clamping nor at the final position. The increase rate of the necessary thrust is consistent with the combination of that of the mechanical advantage and that of deformation force of the tie bars. The two effects of the deformation of the toggle links and the hinge friction should not be neglected during real mold clamping operation. The maximum thrust is underestimated if the effect of the deformation of the toggle links is neglected.

Nomenclature

A_1, A_2, A_c	cross-sectional areas of link 1, link 2, and the tie bar
d_A	vertical distance between point C and Point A
d_E	vertical distance between point C and Point E
E_1, E_2, E_c	Young's Modulus of link 1, link 2, and the tie bar
F_i, (i = 1 – 3)	forces exerted on all the member i
F_{AB}, F_{BC}	axial forces in a single link 1 and a single link 2
F_o	thrust applied to the crosshead
$F_{o,\max}$	maximum value of the thrust F_o during real mold clamping process
F_{cl}	clamping force
L_i (i, = 1 – 3)	distances between points A and B, B and C, and B and E
L_c	length of the tie bar
M_a	mechanical advantage
n_i (i, = 1 – 2)	the number of member i
n_c	the number of tie bars
r_B, r_E	radiuses of pin joints B and E
U_C	displacement of the tailstock platen defined in Eq. (4)
$\overline{U}_C$	parameter defined in Eq. (5)
α, β, ϕ	angles defined in Figs. 2 and 3
α_c, β_c, ϕ_c	angles α, β and ϕ in the position when the moving mold is just in contact with the stationary mold
α_μ, β_μ, ϕ_μ	angles defined in Fig. 3
δ_{AB}, δ_{BC}	axial shortened lengths of links 1 and 2
μ	friction coefficient
ρ_B, ρ_E	friction radiuses of pin joints B and E
$\tilde{(\ )}$	quantity in the state of the final position of mold clamping process

References

Burton, P., *Kinematics and Dynamics of Planner Machinery*, Prentice-Hall, Englewood Cliffs, pp. 424-426 (1979).

Huang, J.H., “Friction, wear, and lubrication,” *Symp. on Development of Design and Electric-Hydraulic Control System for Injection Molding Machines*, pp. 175-194, MIRL, ITER, Hsinchu, Taiwan (in Chinese) (1988).

Smith, A., *How to Choose a Plastics Injection Moulding Machine*, AMI Business Publishing, Bristol, pp. 102-104 (1995).

Wilson, C.E. Sadler, J.P. and Michels, *W.J. Kinematics and Dynamics of Machinery*, Harper and Row, New York, (1983).

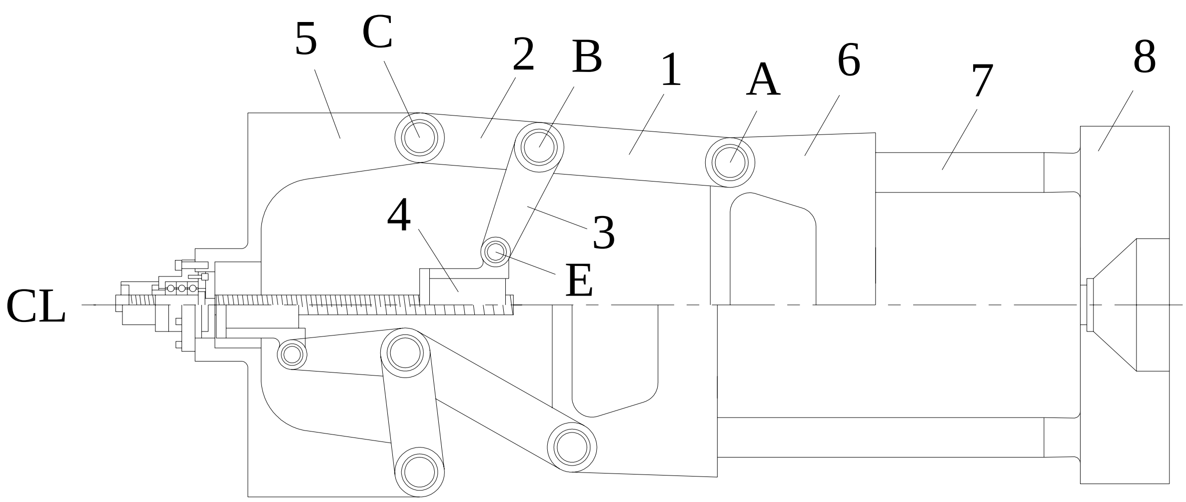

Fig. 1. Four-point double-toggle mold-clamping mechanism.

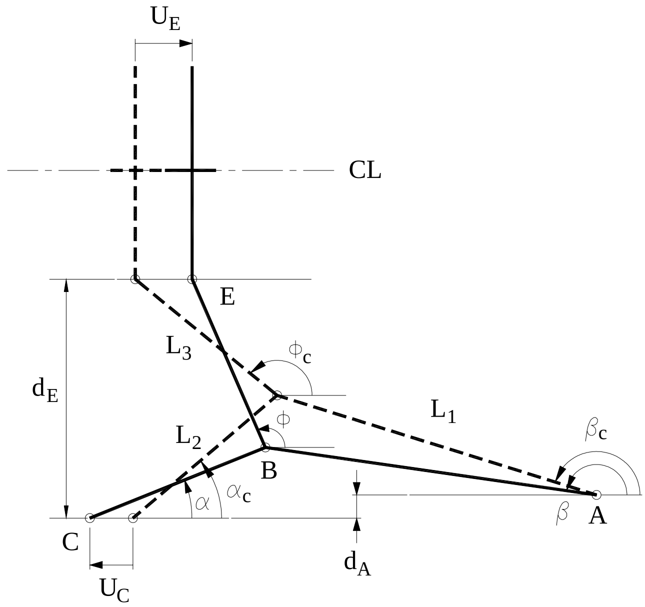

Fig. 2. Geometry of the toggle linkage during real mold clamping.

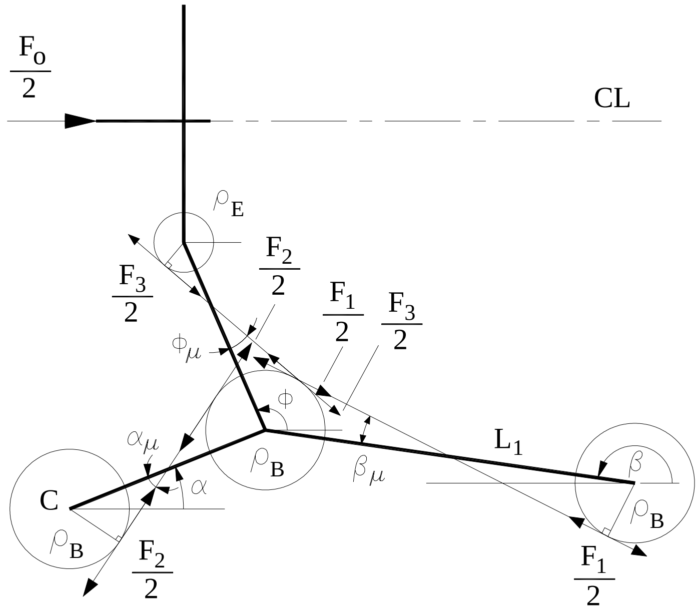

Fig. 3. Toggle linkage subjected to loading during the real mold clamping process.

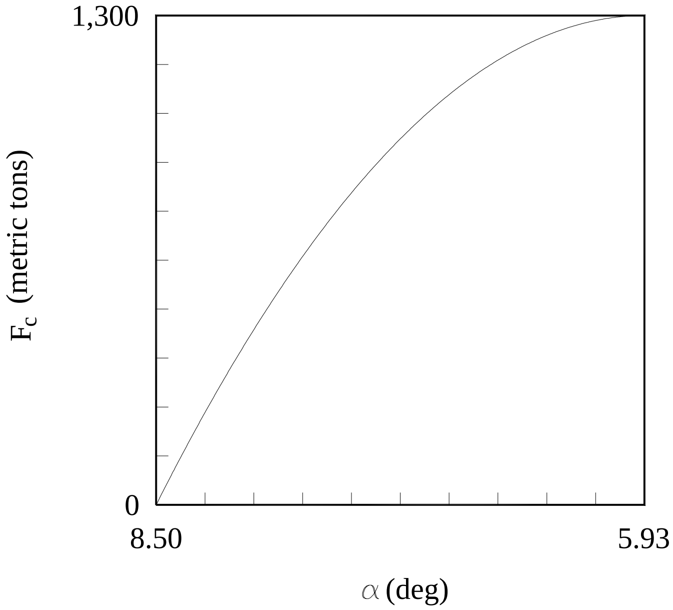

Fig. 4. Total deformational force of the tie bars versus angle α.

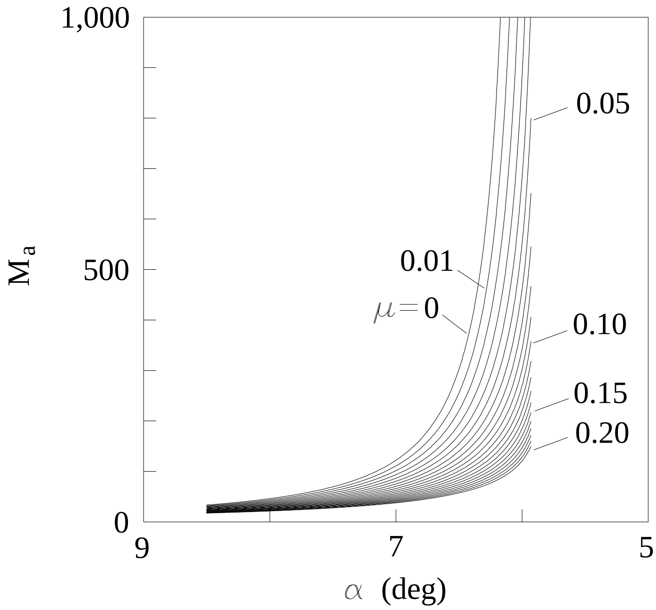

Fig. 5. Mechanical advantage versus angle α.

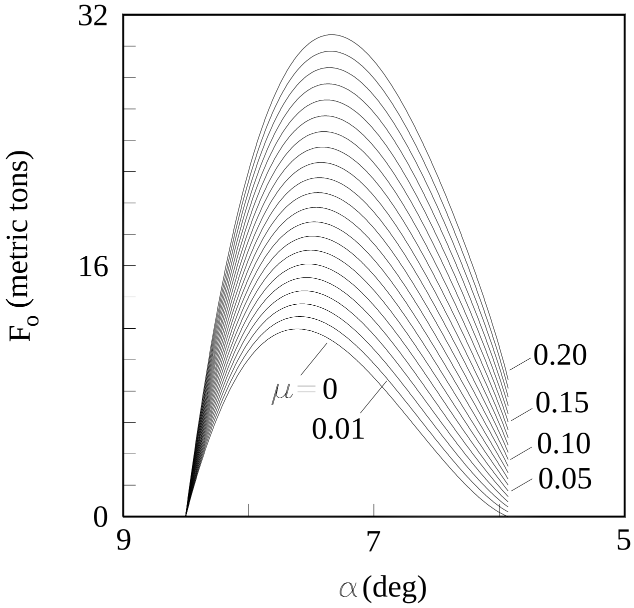

Fig. 6. Thrust applied to the crosshead versus angle α for several frictional coefficients.

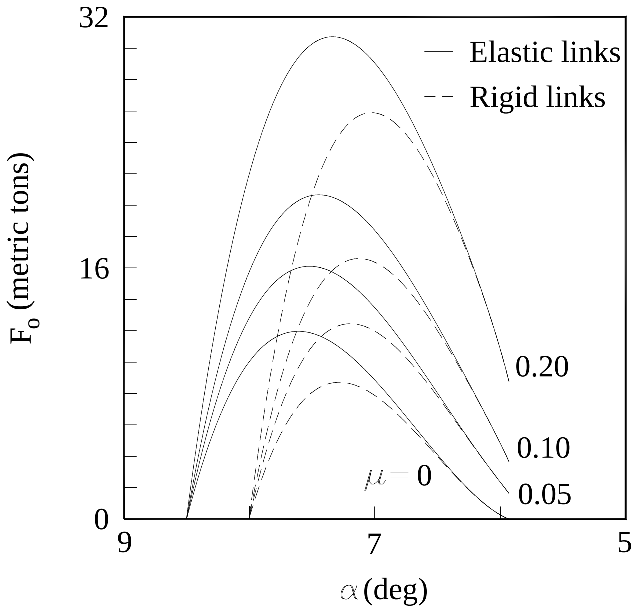

Fig. 7 Thrust applied to the crosshead versus angle α for showing the two effects.

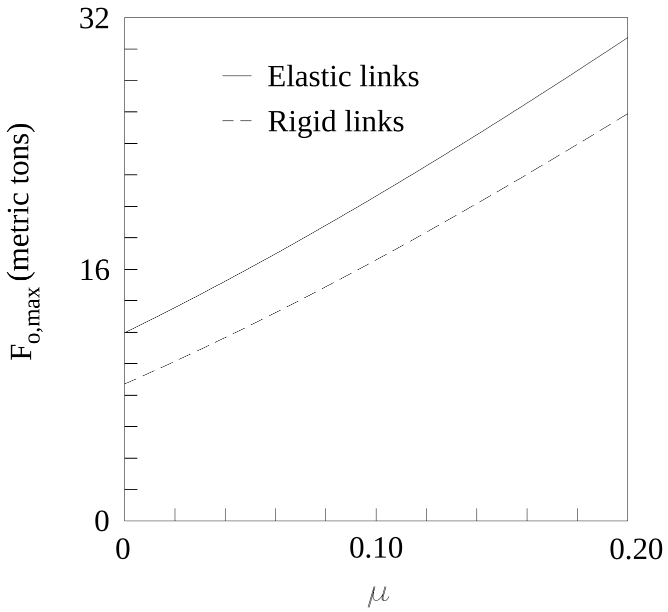

Fig. 8. Maximum thrust applied to the crosshead versus the friction coefficient.